J Therm Anal Calorim (2014) 115:1465–1475
DOI 10.1007/s10973-013-3454-z

Organoclays from alkaline-treated acid-activated clays

Properties and thermal stability

F. Kooli · L. Yan · Sze Xing Tan · Jiae Zheng

Received: 6 May 2013 / Accepted: 1 October 2013 / Published online: 23 October 2013

Abstract The cetyltrimethylammonium hydroxide (C16TMAOH) solution was proposed for the preparation of organoclays. Montmorillonite clay was acid activated at different acid/clay (a/c) (in mass) ratios, then treated with alkaline (sodium hydroxide) solution before being reacted with C16TMAOH solution. The acid activation caused a reduction in the number of cation exchange sites, and hence improved the exfoliation of the silicate sheets at higher pH values. The basal spacing increased significantly from 2.20 to 4.01 nm, and depended on the a/c ratios. The acid-activated clays with a/c ratios greater than 0.3 adsorbed significant amounts of C16TMA cations with a basal spacing of 4.01 nm compared with the non-acid-activated montmorillonite (2.51 nm). Meanwhile, the treatment of NaOH solution yielded clays with similar properties to that of the raw used clay. The XRF data, FT-IR, and ^{29}Si MAS-NMR techniques confirmed that the resulting amorphous silica during the acid activation was dissolved, and accompanied by a dramatical reduction in the surface areas. Similar amounts of C16TMA cations were adsorbed, i.e., close to 1 mmol g^{-1}, with a single basal spacing of 2.52 nm, independently of the treated acid-activated clays. The in-situ powder XRD studies revealed that an increase of the basal spacing to 4.20 nm was observed at intermediate temperatures ranging from 50 to 150 °C for organo-acid-activated clays with basal spacing of 4.01 nm, while a continuous decrease of the basal spacing was observed for organoclays with a basal spacing of 2.52 nm. At higher temperatures greater than 250 °C, the decomposition of the surfactant occurs, and the basal spacing decreases to a value of about 1.4 nm.

Keywords Organoclays · Acid-activation · Thermal stability · Cetyltrimethylammonium · Nanocomposites

F. Kooli (✉)
Department of Chemistry, Taibah University,
PO Box 30002, Medina, Saudi Arabia
e-mail: fkooli@taibahu.edu.sa

L. Yan · S. X. Tan · J. Zheng
Institute of Chemical and Engineering Sciences, 1 Pesek Road,
Jurong Island, Singapore 627833, Singapore

Introduction

The modification of the clay minerals with organic molecules leads to a new type of materials with organophilic properties [1]. These organoclays have found many applications in the preparation of nanocomposites [2], adsorption of nonpolar molecules from contaminated waters [3], the preparation of porous materials [4], sensors, which are used as electrode modifiers, and in catalysis [5, 6]. Clay minerals are layer-lattice silicates, and the layer-lattice silicates are made up of combinations of two structural units: a silicon oxygen tetrahedron, and an aluminum oxygen–hydroxyl octahedron. The clay mineral structure is based on the combination of tetrahedral and octahedral sheets, i.e., 2:1 type consists of one octahedral sheet sandwiched between two tetrahedral sheets; among this kind of family members is montmorillonite clay which was widely used as received without treatment, before their modification with organic cations. However, a chemical treatment of the parent clay minerals could modify the properties of the resulting clays and thereby their organic modification properties [7, 8]. One of the chemical treatment consisted of reacting the clays with inorganic acids (normally HCl or H_2SO_4) at different conditions and concentrations, which is known as acid-activation process [9].

This process resulted in significant changes of chemical composition because of the dissolution of metals ions from the clay structure, and is accompanied by a decrease in the intensity of the basal reflections, as indicated by X-ray diffraction (XRD) techniques [8]. Improvements of the textural and acidic properties of the acid-activated clays were also achieved, with increases in the surface areas, pore volumes, and Brönsted acid sites. Thus, the resulting acid-activated clays exhibited different properties compared with nontreated clay minerals, and they were used extensively in catalysis, as bleaching and decolorizing agents, and adsorbents of inorganic and organic contaminants from polluted waters [10, 11]. However, the reaction of clay minerals with alkaline solution does not lead to the dissolution of the mineral structures [11], and it was used to clean the clay minerals by dissolving the amorphous impurities and phases. Indeed, a Wyoming-type bentonite with pH 13.5 solutions at 35 and 60 °C did not alter the stability of the octahedral sheet along with the composition and the structure of the smectite sheets [12].

The combination of acid treatment of clays and their organic modification provided a potential enhancement in the properties of the clay. The clay mineral presents a proton-rich environment when presented to organic molecules. These organo-acid-activated clays were used as catalysts in some catalytic reactions, and they exhibited higher catalytic yields in the isomerization of alpha-pinene to camphene and limonene [13].

The most studied organoclays were prepared from montmorillonite and cetyltrimethylammonium (C16TMA) cations from its bromide solution. The uptake amounts were controlled by the initial concentration values, means of the ratios of C16TMA moles, and the cation exchange capacity (CEC) of clays [14]. In case of acid-activated clays, the uptake amounts of C16TMA cations from bromide solution decreased with the severity of the acid activation. This fact was related to the decrease of the CEC of the starting clay during the acid activation [15]. The adsorption of C16TMA cations on negatively charged mineral was strongly dependent on pH, because of pH-dependent degree of dissociation of the surfactant itself and on solid phase charge [16]. In fact, when acid-activated clay was reacted with C16TMABr solution, an interlayer spacing of 1.85 nm was obtained. However, by adding NaOH solution during the reaction with C16TMABr, a twofold increase of the interlayer spacing was achieved [17].

Another way to modify the pH of the exchange reaction medium consisted of using the C16TMAOH solution, instead of adding NaOH to C16TMABr solution. In this case, when the acid-activated clays were reacted with the organic solution, different results were obtained, and the organo-acid-activated clays exhibited an interlayer spacing of 4.2 nm with a maximum of 1.20 mmol g^{-1} being intercalated [7]. The expansion of the interlayer spacing was related to the exfoliation properties of acid-activated clay sheets at higher pHs of the C16TMAOH solution [18]. In addition, the use of C16TMAOH solution will decrease the bromide impurities in the organoclays which were found to decrease the thermal stability of quaternary alkyl ammonium-modified clays, and additional purification procedures were needed to remove the bromide anions completely [19].

In this study, we propose to modify the pH of the solid acid-activated clays by a treatment in alkaline solution, i.e., NaOH solution before the reaction with C16TMAOH. The acid-activated materials were fully characterized before and after treatment with NaOH solutions. The adsorption isotherms of C16TMA cations were investigated, and the characterization of the obtained organoclays was reported by different techniques. The chemical stability of the intercalated surfactants and the thermal stability of the organoclays in air atmosphere were also reported.

Experimental

The used montmorillonite clay was received from Nanocor company (USA) under the brand name "polymer grade (PG) montmotmorillonite." The clay mineral exhibited a CEC of 1.42 meq g^{-1} as provided by the supplier. Two procedures for modification of PG clay were followed before the surfactant adsorption or intercalation:

Acid-activation process

A mixture of PG clay and sulfuric acid solution was prepared and kept at 90 °C for overnight. The acid/clay (a/c) ratio calculated was based on dry mass of PG and H_2SO_4 (98 %, as received), and varied between 0.1 and 0.5 [7]. These acid-activated clays were then repeatedly washed with distilled water and dried at room temperature. The samples are noted as APG-X where X indicates the a/c ratio values.

Alkaline (NaOH) treatment

A mixture of 1 gram of raw or acid-activated clay and 25 mL of NaOH solution (3 M) was prepared and stirred at 90 °C overnight. The solid phase was collected by filtration and washed many times with distilled water and then dried at room temperature. The sample will be assigned as BAPG-X, where X corresponds to a/c ratio values. The raw PG clay mineral treated with NaOH solution will be identified as B-PG.

Adsorption of C16TMAOH

The adsorption isotherms of C16TMAOH onto some selected treated clay minerals were obtained from batch experiments, to determine the initial concentration value, leading to higher adsorbed amount of C16TMA cations. 0.1 g of the clay was mixed with 10 mL of surfactant solutions with different initial concentrations. The tubes were placed into mechanical shaker at 120 rpm, and at 25 °C for 18 h. The suspensions were centrifuged for 10 min, and the supernatant was analyzed using UV–Vis spectrophotometer at a wavelength of 195 nm.

Preparation of organoclays

The organoclay-derived APG-X and the BAPG-X clays were prepared by adding 1 gram of clay mineral into 25 mL of C16TMAOH solution with a concentration of 10.2 mM. The exchange reaction was performed at room temperature overnight. The solid phase was separated by filtration and washed with deionized water for several times, and then air dried at room temperature. The samples will be identified as C16TMA-APG-X or C16TMA-BAPG-X.

Characterization techniques

The powder XRD (PXRD) patterns of PG and its derivatives were recorded using Advance 8 diffractometer, from Bruker, with Cu-Kα radiation). The contents of carbon, nitrogen, and hydrogen in the organoclays were estimated using EURO EA elemental analyzer. The x-ray fluorescence (XRF Bruker S4 explorer) was used to determine the chemical composition of PG and its derivatives in terms of percentage of metal oxides. The CECs of the different clays were measured by the micro-Kjedahl method [15]. The modification of PG clay upon acid activation followed by alkaline treatment was investigated by solid NMR and FT-IR spectroscopy. The solid-state nuclear magnetic resonance (NMR) experiments were performed on a Bruker 400 spectrometer operating at ^{29}Si NMR frequency of 78 MHz. A 4-mm magic-angle spinning (MAS) probehead was used with sample-rotation rates of 4.0 kHz for ^{29}Si NMR experiments. Scans numbering 80–100 were accumulated with the recycle delay of 200 s. The ^{29}Si chemical shift is reported with tetramethylsilane (TMS) taken as reference. The FT-IR spectra were collected using a Digilab Excalibur FTS 3000 series spectrometer, the samples were diluted in KBr pellets. The surface area and pore volume of the acid-activated clays and alkaline-treated derivatives were measured by nitrogen sorption using a quantachrome Autosorb 6 instrument. Before analysis, the samples were degassed under vacuum at 120 °C, overnight. Thermogravimetric analysis (TG) features were recorded on a TA Instruments, SDT2960. The measurements were carried out in air flow 100 mL min^{-1} heated from 25 to 800 °C, at a heating rate of 5 °C min^{-1}. The thermal stability of the some selected clays and organoclays was investigated in-situ at real temperatures using Anton Parr heating stage KT450, under air atmosphere, from 25 to 425 °C, and attached to XRD diffractometer described above.

Results and discussion

The first part will describe the modification of starting clay with acid and base solutions.

XRF analysis

The acid treatment of PG clay resulted in two major outcomes: the substitution of the exchangeable cations and the dissolution of metals ions from the clay structure (Table 1). We noticed that Na^+ cations were the most removed cations, because these elements were present in the interlayer spacing and easily exchanged by protons. While Mg^{2+}, Fe^{3+}, and Al^{3+} were not leached easily because they existed in the octahedral sheets of montmorillonite [8]. According to the data presented in Table 1, the dissolution amounts of MgO and Fe_2O_3 occurred to a lesser extent compared with Al_2O_3. The SiO_2 content and the SiO_2/Al_2O_3 ratios increased as a result of dissolution of the other ions.

After treatment of APG-X clays with NaOH solution, significant changes in the XRF data were observed (Table 1). The percentage of Na^+cations in the B-APG-treated clays increased because of the exchange of protons by Na^+ cations from NaOH solution. We noted also a decrease of the percentage of SiO_2, due to the dissolution of amorphous silica, existed in APG clays during the NaOH treatment. This decrease of SiO_2 phase was accompanied by increases in the percentages of MgO and Al_2O_3 in the treated clays. The ratio of SiO_2 to Al_2O_3 was lower compared with APG-X clays, and an average value of 3 was obtained. This value was close to the starting PG clay.

Powder XRD analysis

The PXRD patterns of the PG and its acid-activated counterparts are depicted in Fig. 1. The PG clay mineral was not stable during the acid activation. The PXRD patterns showed a change in crystallinity of smectite phase, the intensity of 001 (ca. 1.54 nm) reflection for APG-X clays decreased and became weaker and broader with the increase of as a/c ratios greater than 0.2 [8]. We noted also that the intensity of 110 and 020 reflection (ca. 0.44 nm) decreased (denoted by an arrow in Fig. 1), indicating that a complete destruction of the clay structure did not occur,

Table 1 The chemical composition (mass %) of the PG clay after acid activation and NaOH solution treatment

Samples	Na_2O	MgO	Al_2O_3	SiO_2	SiO_2/Al_2O_3	CEC/meq g^{-1}
PG	5.4 (4.05)[a]	3.1 (2.19)	21.4 (18.1)	59.7 (51.2)	2.79 (2.82)	1.40
APG-0.1	0.0 (4.34)	2.6 (2.73)	18.2 (21.2)	54.7 (43.8)	3.00 (3.00)	1.20
APG-0.2	0.0 (3.65)	2.3 (1.48)	16.6 (10.8)	58.9 (32.4)	3.54 (3.00)	1.02
APG-0.3	0.0 (4.82)	2.0 (2.46)	14.5 (16.9)	66.5 (48.9)	4.58 (2.91)	0.89
APG-0.4	0.0 (6.25)	1.8 (1.81)	12.7 (13.8))	72.1 (42.1)	5.67 (3.05)	0.78
APG-0.5	0.0 (7.48)	1.0 (1.54)	8.1 (12.7)	83.6 (46.7)	10.32 (3.62)	0.65

[a] Values between brackets corresponds to APG-X clays treated with NaOH solution

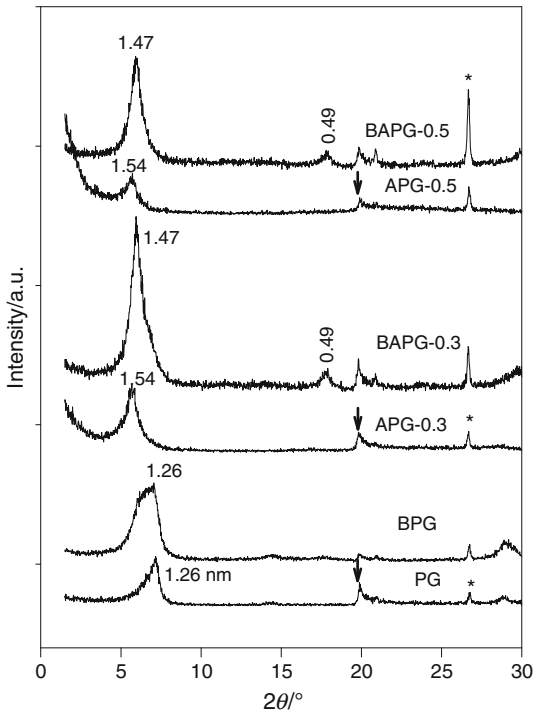

Fig. 1 Powder XRD patterns of PG clay acid activated at selected a/c ratios followed by NaOH treatment. *Asterisk* indicates those corresponding quartz impurities

which is consistent with the chemical compositional data presented in Table 1. The increase in basal spacing from 1.26 nm in raw PG clay, characteristic of a single water layer between the sheets [28] to a value of 1.54 nm in APG for two interlamellar water layers [20], reflects the changes in interlayer cations as a result of the acid treatment.

After the treatment with NaOH solution, the corresponding PXRD patterns are presented in Fig. 1. We noted first a shift of 001 reflection from 1.54 to 1.47 nm, which could be related to the exchange of protons by Na^+ cations with lesser content of water molecules. Similar value of 1.44 nm was reported for montmorillonite clay treated with NaOH solution [21]. The intensity of the 001 reflection (ca. 1.47 nm) was enhanced compared with the starting acid-activated clays, accompanied by the presence of 003 reflection (ca. 0.49 nm), related to the stacking way of the clay mineral sheets and better crystallinity of the resulting BAPG-X clays. The dissolution of the amorphous silica during NaOH treatment was difficult to be detected by PXRD technique. However, its evidence was observed using the FT-IR and ^{29}Si NMR techniques (see below). The formation of new phases was reported when montmorillonite clay was treated with NaOH solution for a period longer than 3 days [21]. In the case of this study, it was difficult to detect new phases. This fact could be related to the short contact time used to treat the materials used in the study, or to the starting clay minerals.

FT-IR spectroscopy

The PG clay exhibited a typical FT-IR spectrum of montmorillonite clay, with intense bands at 3,627 and 3,436 cm^{-1}. These two bands were assigned to the OH stretching vibrations of the structural hydroxyl groups in the clay sheets and the water molecules present in the interlayer, respectively. The band observed at 1,640 cm^{-1} was attributed to the bending vibration mode of water molecules (Fig. 2). The broad bands near 1,110–1,020 cm^{-1} (c.a. 1,024 cm^{-1}) were assigned to complex Si–O stretching vibrations in the tetrahedral sheets. The bands at 920 and 841 cm^{-1} were characteristic of the octahedral sheets. The bands of 525 and 476 cm^{-1} were assigned to Si–O–Al (octahedral Al) and Si–O–Si bending vibrations, respectively [8].

Figure 2 highlights the structural transformation that occurred on the PG clay structure with the increasing a/c ratios. The 1,024 cm^{-1} band shifted to higher wavenumbers, and a band close to 1,100 cm^{-1} was attributed to the Si–O vibrations of the three-dimensional amorphous silica [22]. The presence of amorphous silica was evidenced by the increase in the intensities of the bands near 1210 and 801 cm^{-1}. The bands at 920 and 841 cm^{-1} decreased in intensity, which is in good agreement with the gradual removal of these metals during the acid-activation process [22]. The reduce in intensity of the band at 3,627 cm^{-1} could be attributed to the release of octahedral cations from

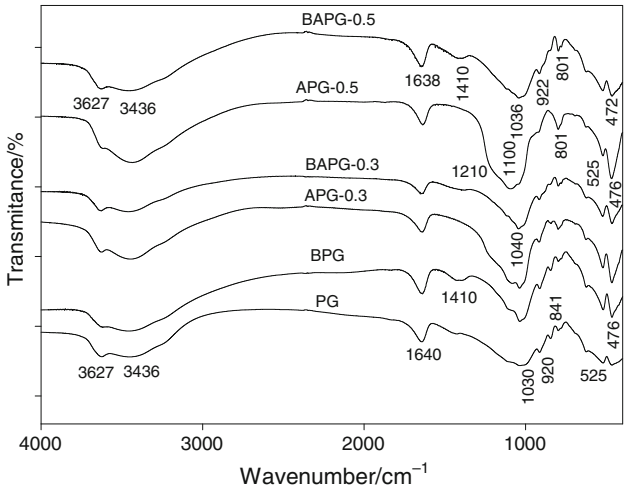

Fig. 2 FT-IR spectra of PG clay acid activated at selected a/c ratios followed by NaOH treatment

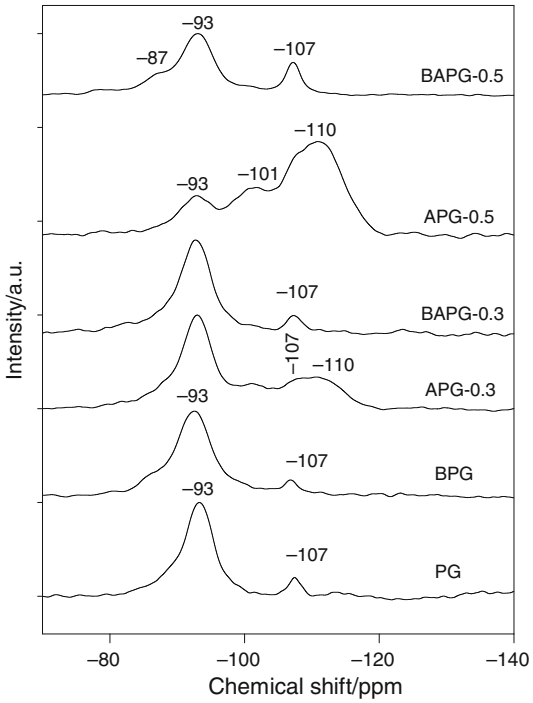

Fig. 3 ^{29}Si MAS NMR spectra of PG clay acid activated at selected a/c ratios followed by NaOH treatment

the structure and to the replacement of interlayer cations by protons. The APG-0.5 clay still retained some clay character, as proved by the incomplete disappearance of the bands at 3,627 and 525 cm^{-1}, in good agreement with the PXRD results.

The FT-IR spectra of selected BAPG-X clays are depicted in Fig. 2. The Si–O environment was affected by the NaOH treatment, as revealed by the changes in the position and shape of the Si–O stretching band in the 1,200–900 cm^{-1} range. The band at 1,100 cm^{-1} almost disappeared and a band at 1,037 cm^{-1} reappeared. The band at 801 cm^{-1} decreased in intensity. These facts were related to the dissolution of the amorphous silica generated during the acid treatment. A broad band at 1,402 cm^{-1} was observed in all the samples, and it could be related to impurities. Regardless the starting APG-X clays, the FT-IR spectra were similar to the parent PG clay with slight decrease of the band at 3,624 and 3,460 cm^{-1} (see Fig. 2).

^{29}Si MAS NMR spectroscopy

The PG clay exhibited an intense resonance band at −93 pm, assigned to silicon in Q^3 (0Al) units, i.e., SiO_4 groups cross linked in the tetrahedral sheets with no aluminum in the neighboring tetrahedral (Fig. 3) [23]. Additional band at -107 ppm was assigned to silica impurities as detected by PXRD technique. When the acid activation progresses, the intensity of the silicon band at −93 ppm decreased progressively, because of the destruction of the clay sheets, and a progressive increase of the bands in the range of −100 to −110 ppm was observed. These bands were assigned to silica phase formed during the progress of the acid activation, with no aluminum being present and is generally labeled Q^4(0Al) [24, 25].

When these materials were treated by NaOH solution, a dramatical change in the spectra was observed (Fig. 3). The broad resonance bands in the range −100 to −110 ppm disappeared for BAPG-0.2 to BAPG-0.5 clays, because of the dissolution of the amorphous silica formed during the acid-activation process by NaOH solution. Only a sharp band at −107 ppm was detected as we have reported for the parent PG clay. The intensity of the latter increased with the increase of a/c ratios, and was the highest in case of BAPG-0.5, with additional band at −87 ppm. The observation was in good agreement with the data of FT-IR technique. However, its intensity was lower than the one at −93 ppm. On the other hand, the band at −93 ppm was clearly detected for all the BAPG-X clays, and its intensity was much higher compared with the starting APG-X clays. The overall spectra of the BAPG clays were similar to those of the starting PG clay with slight variation in the intensities of the characteristic resonance bands at −93 and −107 ppm, respectively (see Fig. 3).

Textural properties

The specific surface area (SSA), pore volumes, and the average pore diameters of different samples are reported in Table 2. The acid-activation process induced an increase of the SSA values, and it depended on the extent of the acid-activation severity. Indeed, APG-X clays exhibited higher SSA values compared with the parent PG one, Similar

Table 2 Textural properties of PG clay and its activated counterparts with acid and bases solutions

Samples	SSA/m^2 g^{-1}	TPV/cm^3 g^{-1}	APS/Å
PG	5 (10)[a]	0.031 (0.016)	267 (223)
APG-0.1	127 (11)	0.126 (0.031)	40 (358)
APG-0.2	151 (13)	0.224 (0.097)	59 (233)
APG-0.3	216 (12)	0.227 (0.030)	42 (162)
APG-0.4	234 (10)	0.350 (0.053)	63 (201)
APG-0.5	273 (12)	0.458 (0.02)	67 (189)

SSA is the specific surface area, *TPV* is total pore volume, *APS* stands for average pore size

[a] Values between brackets corresponds to APG-X clays treated with NaOH solution

results were reported for other montmorillonite and saponite clays [7, 26]. Indeed, APG-0.5 exhibited the highest surface area of 273 m^2 g^{-1}. These values were close to that reported for acid-activated clays [8]. The increase of the SSA was attributed to the presence of the amorphous silica formed during the acid activation. The increase of the pore volume (at $P/P_o = 0.95$) was related to the alteration of the mesopores formed between the particles, and accompanied by an increase of average pore diameter [12]. After the NaOH treatment of the acid-activated clays, the SSA values dramatically decreased due the dissolution of the amorphous silica, and an average of 10 m^2 g^{-1} was obtained (Table 2). We noted that the pore volume and the average pore size values were also affected. This fact might be related to the organization of the clay particles during the base treatment, and the dissolution of the amorphous silica phase. The obtained values were lower than that of the starting clay and close to that of the B-PG clay.

This following section will describe the characterization of the resulting organoclays derived from the above modified clays.

C16TMA Adsorption isotherms

The adsorption isotherms of PG, APG-0.3, and B-APG-0.3 are presented in Fig. 4. The amount of intercalated surfactant molecules increased linearly and eventually reached a plateau as the initial concentrations of C16TMAOH increased. The maximum amounts of C16TMA adsorbed were close to 1.11, 1.45, and 1.02 mmol g^{-1} for PG, APG-0.3, and B-APG-0.3, respectively. At lower concentrations, the used clay minerals displayed a high affinity for surfactants, because of facile exchange of Na^+ cations by C16TMA cations. In this case, the adsorption process was primarily driven by cation exchange [27]. However, at higher concentrations, the APG-0.3 adsorbed more surfactant molecules than the raw PG and BAPG-0.3 clays. These data seemed surprising, since, the acid activation

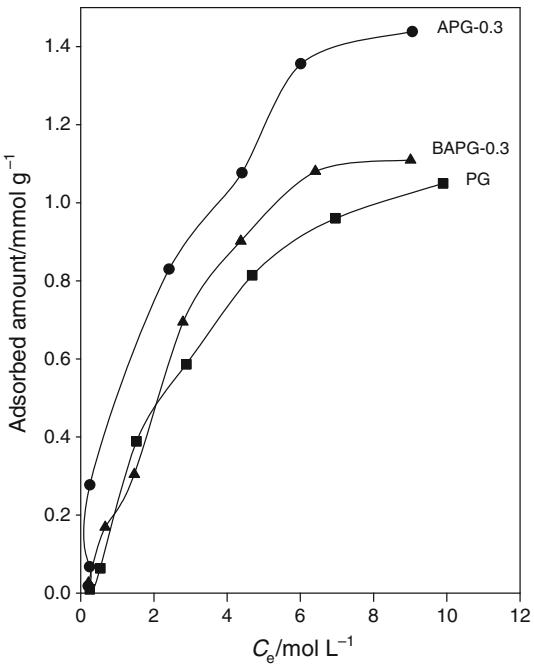

Fig. 4 Uptake amount of C16TMA cations by PG clay acid activated at a/c ratio of 0.3, and NaOH-treated acid-activated clay

reduced the CEC of PG clay (Table 1); as a result, the uptake amount should decrease. One possible explanation could be related to the input of the amorphous-like silica phase for the adsorption of C16TMA cations [28], which possibly overcame the input of the clay mineral itself. However, a major part of this phase was dissolved during the reaction with C16TMAOH, as we had reported previously [7]. These data indicated that the BAPG-X clays behave in a similar manner as the original nontreated PG clays.

C, H, and N analysis

The total C, H, and N analysis data of the organoclays prepared from PG and APG-X clays minerals are presented in Table 3, which confirmed the results deduced from the isotherm adsorptions. The adsorbed amounts of surfactants exceeded the CEC values, as acid activation became more severe, and it remained quite constant at 1.45 mmol g^{-1} for a/c ratios greater than 0.3. Similar behavior was reported for another acid-activated montmorillonite clay from different sources with a maximum of 1.26 mmol g^{-1}. The cationic surfactants can be adsorbed onto the montmorillonite clay surface by two mechanisms: cation exchange, and hydrophobic bondings [29]. As a result, the amount of adsorbed surfactant may significantly exceed the ion exchange capacity [30]. The excessive surfactant may be located either in the vicinity of the clay surface or between the adsorbed organic layers. In our case, the increase of the C16TMA content from hydroxide solution

Table 3 C, H, and N analysis (in mass %) of organoclays derived from PG treated with acid and bases solutions

Samples	C	H	N	IA/ mmol g^{-1}
C16TMA-PG	24.9 (23.0)[a]	5.11 (4.83)	1.24 (1.57)	1.10 (1.00)
C16TMA-APG-0.1	26.5 (23.0)	5.59 (4.83)	1.47 (1.68)	1.16 (1.00)
C16TMA-APG-0.2	28.2 (22.3)	6.07 (4.87)	1.54 (1.57)	1.24 (0.98)
C16TMA-APG-0.3	30.1 (22.1)	6.27 (4.80)	1.48 (1.71)	1.32 (0.97)
C16TMA-APG-0.4	33.8 (22.4)	6.83 (4.87)	1.60 (1.80)	1.45 (0.98)
C16TMA-APG-0.5	32.7 (23.7)	6.87 (5.00)	1.78 (1.81)	1.43 (1.05)

IA is intercalated amount

[a] Corresponds to organoclays prepared after treatment of APG-X clays with NaOH solution

was not related only to cation exchange reaction, but it was related also to the exfoliation of the clay sheets at higher pHs of the surfactant solution, and the adsorption of C16TMA cations at both sides of the separated sheets, as we had proposed previously [18].

The C16TMA-BAPG-X clays exhibited different behaviors: they adsorbed the same surfactant amounts, independent of the starting BAPG-X clays (Table 3), with an average of 1 mmol g^{-1}. The uptake amounts of C16TMA cations by the different BAPG-X clays were lower than those of the corresponding APG-X counterparts, and were close to those of the starting PG clay. These data could indicate that NaOH treatment has modified the charge characteristic of the acid-activated clays, particularly the one which affected the exfoliation properties of the clay sheets at higher pH values. In this case, the intercalation of C16TMA cations occurred via cation exchange reaction.

Powder XRD

The PXRD patterns of the organo-acid-activated clays are presented in Fig. 5. The C16TMA-PG and C16TMA-APG-0.1 exhibited interlayer spacings of 2.52 and 2.78 nm, respectively. However, it increased dramatically to a value of 4.01 nm for C16TMA-APG-X at a/c ratios higher than 0.2. The detection of the second order of the organoclay phase (1.97–2.01 nm) indicated a well-ordered nature of the C16TMA cations in these materials. The expansion of the interlayer spacing was related to the amount of C16TMA cations and its orientation within this spacing. In case of C16TMA-BAPG-X clays, the PXRD patterns exhibited the same interlayer spacing of about 2.52 nm

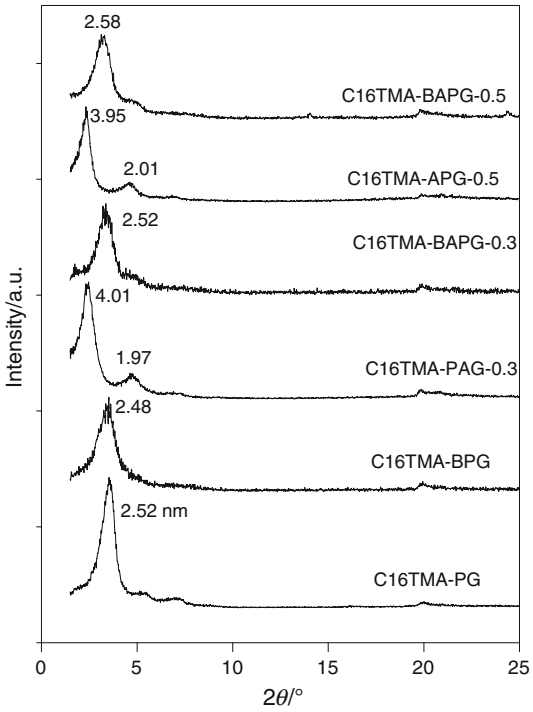

Fig. 5 Powder XRD patterns of organoclays prepared from PG clay acid activated at selected a/c ratios followed by NaOH treatment

(Fig. 5), and a decrease of the interlayer spacing from 4.01 to 2.51–2.58 nm was observed. This decrease was related to the less intercalation of C16TMA cations as reported in Table 3 [31].

The PXRD data indicated that the BAPG-X clays behave in the similar manner as the parent PG clay. Indeed, the value of 2.52 nm was close to that obtained for the C16TMA-PG, the organoclay prepared from the raw PG clay (2.52 nm). The variation of the basal spacing of the organoclays resulted in different orientations of the C16TMA cations in the interlayer region. [31] The C16TMA cations could be described as a nail, the trimethylammonium cation as the head, and the C16 chain as the tail. The dimension of the C16TMA cation was estimated in the order of 2.20 nm [32], and taking into account the basal spacing of fully dehydrated montmorillonite clay (0.96 nm [33],) the basal spacing of 2.51-nm phase corresponds to a gallery height of 1.55 nm, and this was assigned to the formation of paraffin monolayer. However, the basal spacing of 4.01-nm phase corresponded to an interlayer gallery of 3.05 nm. This value exceeded the length of the C16TMA cation (2.20 nm), indicating that the intercalated surfactant cations adopted a tilted bilayer structure. For a simple case of a bilayer structure where methylene chains are exclusively all-trans and interdigitation is absent, the tilt angle is in the range of 37°–43° (dependent on the size of the organic cation) with respect to the layers [30].

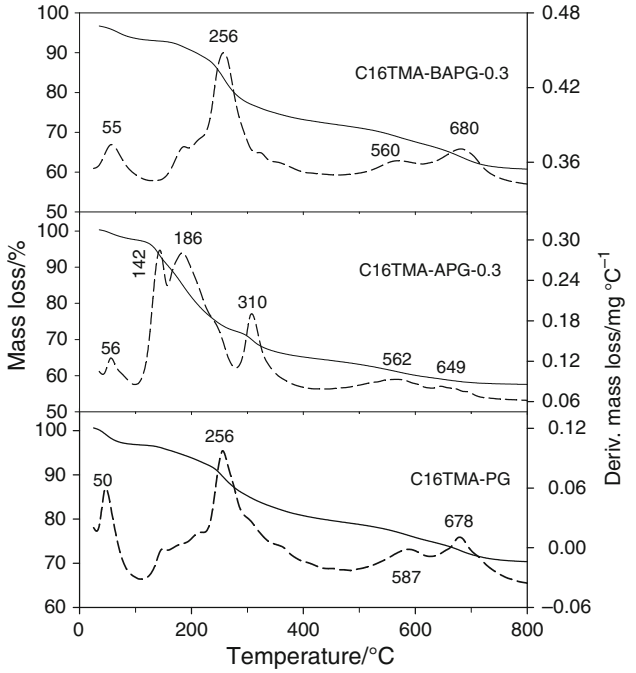

Fig. 6 TG (*solid line*) and DTG (*dashed line*) features of different organoclays

TG

TG and DTG analysis were performed to study the thermal stability of the organotreated clays. The C16TMA-PG material exhibited a mass loss of 17 % related to the C16TMA cations in the temperature ranging from 200 to 440 °C with the maximum temperature being 256 °C (Fig. 6) [34]. While, C16TMA-APG-X exhibited different features (C16TMA-APG-0.3 is shown as an example) with different mass loss steps associated to different release steps of the C16TMA cations, with a starting temperature of 100 °C. The DTG curves showed three maximum temperature sets at 142, 186, and 310 °C for the release of the intercalated surfactants (Fig. 6) [35]. The percentage mass loss (32 %) was higher than that of the C16TMA-PG material. The mechanism of the C16TMA cations degradation was affected by the environment of the C16TMA cations within the clay sheets [19, 36]. However, The DTG curves of the C16TMA-BAPG-X clays (C16TMA-BAPG-0.3 is shown as an example) indicated that the way of losing the surfactants was modified compared with C16TMA-APG-X clays, and was similar to the organoclay prepared from the raw PG clay (C16TMA-PG, Fig. 6). Indeed, the DTG curve exhibited similar feature than C16TMA-PG clay, with a mass loss percentage of 14 % in the temperature range between 220 and 440 °C, with a maximum temperature at 256 °C (Fig. 6). These data confirmed that the properties of the acid-activated clay were modified after the NaOH treatment, and consequently affected the decomposition mechanism of the C16TMA surfactants. The last mass-loss step at temperatures greater than 620 °C was associated to complete oxidation of the residual charcoal in the organoclays. We noted that the percentage mass loss related to water molecules decreased up to 4 % with a shift at lower temperature of 50 °C, thus confirming that the water molecules were present on the surface of the organoclays and not in the interlayer spacing [37], and also confirming the surface affinity change (from hydrophobicity to hydrophilicity) of the modified clay minerals.

Chemical stability of the intercalated C16TMA cations

The chemical stability of the intercalated C16TMA cations for selected organoclays was investigated by reacting the intercalated C16TMA-clays with NaOH or HCl solutions (0.1 M). The results indicated that a displacement of the intercalated C16TMA cations was not achieved by Na^+ cations or protons. The PXRD patterns exhibited similar basal spacings before and after reaction with NaOH or HCl solutions, with some variations in the degree of crystallinity. Similar results were reported for shorter tetra-alkylammonium intercalated clays, treated with acidic solutions [38]. However, in case of different organosilicates, i.e., C16TMA-magadiites, the C16TMA cations were easily exchanged by protons in acidic solutions. These data indicated that the chemical compositions of the silicate layers affected the interactions between the C16TMA cations and the silicate sheets, and thereby its replacement with other cations [39].

Thermal stability of organoclays

The thermal stabilities of the acid and alkali treatment of clays were also studied by in-situ XRD technique in air atmosphere. The pristine PG clay was stable at temperatures less than 100 °C with a decrease of the basal spacing from 1.26 to 0.98 nm. This decrease was related to loss of intercalated and hydrated water molecules between the interlayer spacings [40]. As regards APG-0.5 clay, it exhibited a different behavior with higher stability and basal spacing of 1.31 nm when heated at temperatures ranging from 100 to 400 °C (Fig. 7). This difference in basal spacing could indicate the presence of some silica species between the clay mineral layers which acted as pillars and prevented the collapse of the clay mineral layers [15]. While the AC-PG-0.3 clay showed an intermediate behavior, both interlayer spacings at 0.98 and 1.34 nm were obtained during the calcination process.

After a treatment with NaOH, the BAPG-0.5 exhibited different thermal stability properties: the phase at 1.34 nm was not detected even at lower temperatures of 100 °C, and

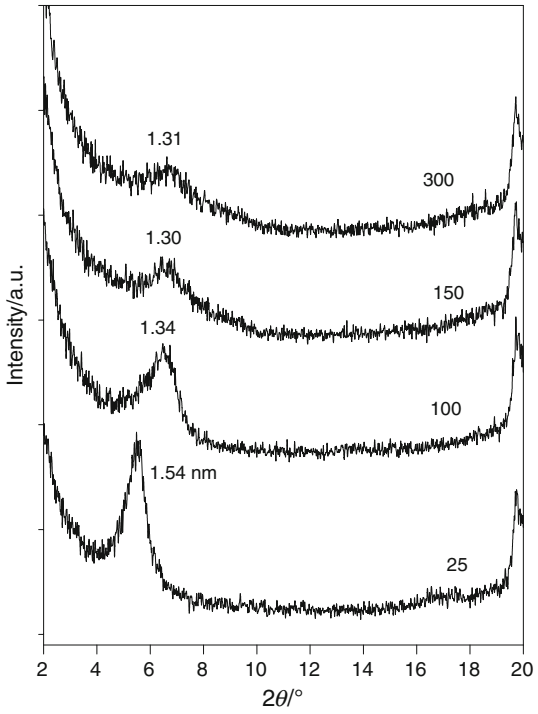

Fig. 7 In-situ X ray diffraction patterns of APG-0.5 clay calcined at different temperatures

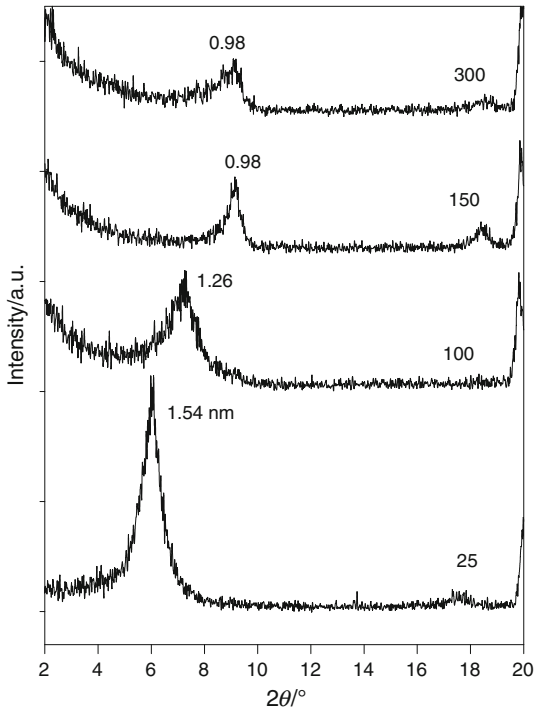

Fig. 8 In-situ X ray diffraction patterns of BAPG-0.5 clay calcined at different temperatures

the basal spacing of BAPG-X clays heated at 150 °C had shrunk to 0.98 nm (Fig. 8). This fact could indicate that the possible pillaring silica species were eliminated during the alkali treatment as supported by ^{29}Si NMR and FT-IR studies. In addition, BAPG-X clay exhibited similar properties as the starting PG clay.

In case of C16TMA-PG, the interlayer spacing of 2.21 nm was stable up to 200 °C, and a shift of the interlayer spacing from 2.28 to 1.92 nm was observed between 215 and 250 °C. On the other hand, a complete shrinkage of the interlayer spacing at 1.44 nm occurred at temperature greater than 250 °C because of the C16TMA decomposition as indicated by TG curve. The layered structure was still preserved with a basal spacing of 1.30 nm at 400 °C. Similar behavior was reported for organoclays prepared from different montmorillonites [34].

The organo-acid-activated clays (C16TMA-APG-X) showed higher thermal stability up to 250 °C compared with the C16TMA-PG organoclays. An average value of 1.90 nm was obtained. However, at temperatures greater than 250 °C, the interlayer spacing shrank to 1.52 nm because of the complete decomposition of the surfactants, which is in good agreement with TG data (Fig. 9). In addition to this phase (1.90 nm), the PXRD pattern of C16TMA- APG-0.5 exhibited an additional reflection at 4.50 nm. This phase was detected even at 300 °C, and it could be related to the formation of three-dimensional network of aluminosilicate after calcination at higher temperatures (Fig. 9). Previous studies related to alkylammonium clays indicated an initial increase of the basal spacing when they were heated from 50 to 100 °C. This was related to melting of the intercalated surfactant, creating a fluid-like environment between the layers where the surfactants adopted a disordered conformation [14, 35, 36]. We have noted an increase in the basal spacing only at 150 °C for the C16TMA-APG-X with X values higher than 0.3, whereas a gradual decrease was only observed for the other organoclays from room temperature till 215 °C.

In general, the C16TMA-BAPG-X clays exhibited different behavior from that of the C16TMA-APG-X clays. The in-situ XRD diffraction of C16TMA-BAPG-0.5 presented as an example is shown in Fig. 10. The starting sample exhibited mainly a reflection at 2.20 nm at temperatures less than 200 °C, and then shifted to higher angles (phase of 1.92 nm) when treated at 215 °C. A significant decrease of the interlayer spacing from 1.92 to 1.40 nm occurred in the range of 215–250 °C, with a continuous shrinkage of the interlayer spacing from 1.40 to 1.32 nm occurring at higher temperatures. This value was higher than the value corresponding to the completely collapsed clay sheets (0.96 nm). This difference was due to the presence of remaining charcoal material between the clay sheets [34]. This behavior was similar to that of the C16TMA-PG clay, and it indicated that the treatment of

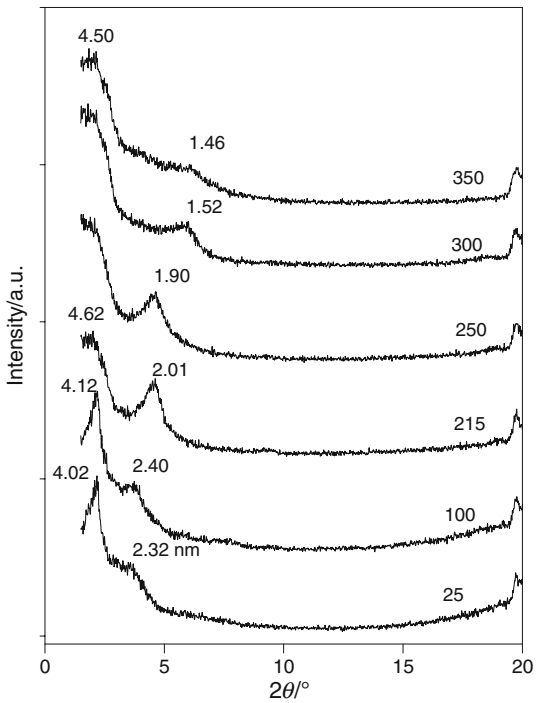

Fig. 9 In-situ X ray diffraction patterns of C16TMA-APG-0.5 clay calcined at different temperatures

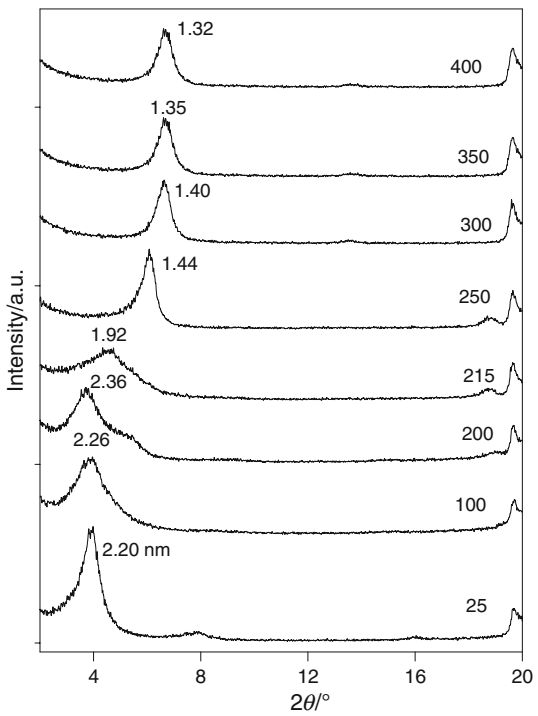

Fig. 10 In-situ X ray diffraction patterns of C16TMA-BAPG-0.5 clay calcined at different temperatures

the acid-activated clays by NaOH solution resulted in materials with characteristics close to those of the starting PG clay.

Conclusions

The activation of PG clay with acid solution led to a decrease of the percentage of metal oxides, except for silica, and to the modifications of its properties, particularly the intercalation of C16TMA cations from hydroxide solution. The amount of intercalated and the orientations of C16TMA cations depended on the acid-activation level with a maximum of 1.45 mmol g^{-1} of clay and interlayer spacing of 4.01 nm for materials prepared from APG-X with a/c ratios higher than 0.3. Further treatment of these acid-activated clays with NaOH solution led to the dissolution of amorphous silica material, and the resulting clays had similar properties to those of the starting PG clay, and consequently, the uptake amounts of C16TMA cations were close to 1.0 mmol g^{-1} value of clay, where only one interlayer spacing of 2.52 nm was obtained. The thermal stability properties of the APG-X clays and their organoclays' derivatives were improved. However, after alkaline treatment, the thermal properties of the derived organoclays were similar to those of the organoclays prepared from the nontreated parent clay.

Acknowledgements The financial support from Taibah University (Grant 429/220) and the technical support from the Institute of Chemical and Engineering Sciences, Agency of Science, Technology and Research (A-STAR), Singapore are highly appreciated.

References

1. Van Oss CJ, Giese RF. The hydrophilicity and hydrophobicity of clay minerals. Clays Clay Miner. 1995;3:474–7.
2. de Paiva LB, Morales AR, Valenzuela Diaz FR. Organoclays: properties, preparation and applications. Appl Clay Sci. 2008;42:8–24.
3. Barreto EP, Lemos MS, Aranha IB, Büchler PM, Dweck J. Partially exchanged organophilic bentonites Part II. Phenol adsorption. J Therm Anal Calorim. 2011;105:915–20.
4. Kooli F, Hian PC, Weirong Q, Alshahateet SF, Fengxi C. Effect of the acid-activated clays on the properties of porous clay heterostructures. J Porous Mater. 2008;13:319–24.
5. Manisankar P, Selvanathan G, Vedhi C. Determination of pesticides using heteropolyacid montmorillonite clay-modified electrode with surfactant. Talanta. 2008;68:686–92.
6. Wallis PJ, Chaffee AL, Gates WP, Patti AF, Scott JL. Partial exchange of Fe(III) montmorillonite with hexadecyltrimethylammonium cation increases catalytic activity for hydrophobic substrates. Langmuir. 2010;26:4258–65.
7. Kooli F, Khimyak YZ, Alshahateet SF, Chen F. Effect of the acid activation levels of montmorillonite clay on the cetyltrimethylammonium cations adsorption. Langmuir. 2005;21:8717–23.
8. Komadel P. Chemically modified smectites. Clay Miner. 2004;38:127–38.
9. Hussin F, Aroua MK, Wan Daud WMA. Textural characteristics, surface chemistry and activation of bleaching earth: a review. Chem Eng J. 2011;170:90–106.
10. Breen C, Zahoor FD, Madejova J, Komadel P. Characterization and catalytic activity of acid-treated, size-functionated smectites. J Phys Chem B. 1997;27:5324–31.

11. Didi M, Makhoukhi B, Azzouz A, Villemin D. Colza oil bleaching through optimized acid activation of bentonite. A comparative study. Appl Clay Sci. 2009;42:336–44.
12. Jozefaciuk G, Bowanko G. Effect of acid and alkali treatments on surface areas and adsorption energies of selected minerals. Clays Clay Miner. 2002;50:771–83.
13. Taubald H, Bauer A, Schafer T, Geckeis H, Satir M, Kim JI. Experimental investigation of the effect of high-pH solutions on the Opalinus Shale and the Hammerschmiede smectite. Clay Miner. 2002;35:515–24.
14. Zhu J, Shen W, Ma Y, Ma L, Zhou Q, Yuan P, Liu D, He H. The influence of alkyl chain length on surfactant distribution within organo-montmorillonites and their thermal stability. J Therm Anal Calorim. 2012;109:301–9.
15. Kooli F, Liu Y, Alshahateet SF, Messali M, Bergaya F. Reaction of acid activated montmorillonites with hexadecyl trimethylammonium bromide solution. Appl Clay Sci. 2009;43:357–63.
16. Rutland MW, Parker JL. Surfaces forces between silica surfaces in cationic surfactant solutions. Langmuir. 1994;10:1110–21.
17. Kooli F, Magusin PCMM. Adsorption Studies of cetyltrimethylammonium ions on an acid-activated smectite, and their thermal stability. Clay Miner. 2005;40:233–43.
18. Kooli F. Exfoliation properties of acid-activated montmorillonites and their resulting organoclays. Langmuir. 2009;25:724–30.
19. Davis RD, Gilman JW, Sutto TE, Callahan JH, Trulove PC, De Long HC. Improved thermal stability of organically modified layered silicate. Clays Clay Miner. 2004;52:171–9.
20. Ferrage E, Lanson B, Sakharov BA, Drits VA. Investigation of smectite hydration properties by modeling of X-ray diffraction profiles. Part 1. Montmorillonite hydration properties. Amer Miner. 2005;90:1358–74.
21. Gates PW, Bouazza A. Bentonite transformations in strongly alkaline solutions. Geotextiles Geomembranes. 2010;28:206–18.
22. Madejova J, Bujdák J, Janek M, Komadel P. Comparative FT-IR study of structural modifications during acid treatment of dioctahedral smectites and hectorite. Spectrochim Acta A. 1998;54: 06–1397.
23. Sanz J, Robert JL. Influence of structural factors on ^{29}Si and ^{27}Al NMR chemical shifts of 2:1 phyllosilicates. Physic Chem Miner. 1992;19:39–45.
24. Breen C, Madejova J, Komadel P. Correlation of catalytic activity with infra-red, ^{29}Si MAS NMR and acidity data for HCl-treated fine fractions of montmorillonites. Appl Clay Sci. 1995;10:219–30.
25. Wu P, Ming C. The relationship between acidic activation and microstructural changes in montmorillonite from Heping, China. Spectrochim. Acta A. 2006;63:85–90.
26. Vicente MA, Suárez M, López-González JD, Bañares-Muñoz MA. Characterization, surface area, and porosity analyses of the solids obtained by acid leaching of a saponite. Langmuir. 1989;12:566–72.
27. Lee SY, Kim SJ. Adsorption of naphthalene by HDTMA modified kaolinite and halloysite. Appl Clay Sci. 2002;22:55–63.
28. Santanu P, Kartic CK. A review on experimental studies of surfactant adsorption at the hydrophilic solid-water. Adv Colloid Interface Sci. 2004;110:75–95.
29. Xu SH, Boyd SA. Alternative model for cationic surfactant adsorption by layer silicates. Environ Sci Technol. 1995;29:3022–8.
30. Yui T, Yoshida H, Tachibana H, Tryk DA, Inoue H. Intercalation of polyfluorinated surfactant into clay minerals and the characterization of the hybrid compounds. Langmuir. 2002;18:891–6.
31. Silva SML, Leite IF, Soaras.APS, Carvalho LH, Rapso CMO, Malta OML. Characterization of pristine and purified organobentonites. J Therm Anal Calorim. 2010;100:563–9.
32. Zhu R, Zhu L, Zhu J, Xu L. Structure of cetyltrimethylammonium intercalated hydrobiotite. Appl Clay Sci. 2008;42:224–31.
33. Bayram H, Onal M, Ytlmaz H, Sarikaya Y. Thermal analysis of a white calcium bentonite. J Therm Anal Calorim. 2010;101:873–9.
34. Kooli F. Effect of C16TMA contents on the thermal stability of organo-bentonites: in situ X-ray diffraction analysis. Thermochim Acta. 2013;551:7–13.
35. Park Y, Ayoko GA, Kristof J, Horvath E, Frost RL. A thermoanalytical assessment of an organoclay. J Therm Anal Calorim. 2012;107:611–8.
36. Xie W, Gao Z, Pan WP, Hunter D, Singh A, Vaia R. Thermal degradation chemistry of alkyl quaternary ammonium montmorillonite. Chem Mater. 2001;13:2979–90.
37. Lapides I, Borisover M, Yariv S. Thermal analyis of hexadecyltrimethylammonium Montmorillonites Part 1. Thermogravimetry, carbon and hydrogen analysis and thermo-IR spectroscopy analysis. J Therm Anal Calorim. 2011;105:921–9.
38. Pálková H, Jankovič L, Zimowska M, Madejová J. Alterations of the surface and morphology of tetraalkyl-ammonium modified montmorillonites upon acid treatment. J Colloid Interface Sci. 2011;363:213–22.
39. Kooli F, Yan L. Thermal stable cetyl trimethylammonium-magadiites: influence of the surfactant solution type. J Phys Chem C. 2009;113:1947–52.
40. Ursu AV, Jinescu G, Gros F, Nistor ID, Miron ND, Lisa G, Silion M, Djelveh G, Azzouz A. Thermal and chemical stability of Romanian bentonite. J Therm Anal Calorim. 2011;106:965–71.